This is the Pre-Published Version.
J. Fang*, Y. Xue, X. Huang*, J. Wang, S. Zhao, X. He, L. Zhao (2019) *Dripping and Fire Extinction Limits of Thin Wire: Effect of Pressure and Oxygen*, Combustion Science and Technology. https://doi.org/10.1080/00102202.2019.1658578
This is an Accepted Manuscript of an article published by Taylor & Francis in Combustion Science and Technology on 25 Aug 2019 (Published online), available online: http://www.tandfonline.com/10.1080/00102202.2019.1658578.

Dripping and Fire Extinction Limits of Thin Wire: Effect of Pressure and Oxygen

Jun Fang[1],Yue Zhang[1], Xinyan Huang[2,*], Yan Xue[1], Jingwu Wang[1], Siwei Zhao[1], Xuanze He[1], Luyao Zhao[1]

[1]*State Key Laboratory of Fire Science, University of Science and Technology of China, Hefei, Anhui, China*

[2]*Department of Building Services Engineering, The Hong Kong Polytechnic University, Kowloon, Hong Kong*

***Corresponding authors:** Jun Fang fangjun@ustc.edu.cn, and Xinyan Huang xy.huang@polyu.edu.hk*

Abstract: Fire safety is a significant concern in aviation as well as space travel and settlement, where reduced pressure and raised oxygen concentration are used. Electrical wire has been identified as a major fire hazard in these special applications. Besides the flame spread in wire insulation, the molten insulation surrounded by a flame can drop due to gravity. Such flame dripping in wire fire represents an important and different type of fire risk but has been ignored. To better evaluate the aircraft fire risk, we conduct laboratory experiments with thin nichrome and copper wire samples under various ambient oxygen concentration and pressure. For the first time, we find two important limits for wire fire, the upper dripping limit and the lower extinction limit, as a function of pressure and oxygen concentration. Between these two limits, both the spread of flame and dripping accompanied by flame occur, defining the worst fire-wire scenario. In the "normoxic" atmosphere (i.e., oxygen partial pressure of 21 kPa), dripping occurs to the copper wire below 70 kPa, but never to the low-conductivity nichrome wire. The mass of drip is controlled by the force balance between gravity, surface-tension, and inertia forces, and it is insensitive to the wire size and core material while changes with the ambient condition. At the extinction limit, the wire core changes from a heat source to a heat sink as the oxygen concentration is decreased.

***Keywords**: Thin Wire; Normoxic; Combustion Limit; Flame Spread; Drip Mass*

1. Introduction

Fire safety in the reduced pressure is an important concern for aviation and space travels [1–4], and the electrical wire has been identified as a major fire hazard. A deep understanding of fire phenomena on electrical wires in the reduced pressure and raised oxygen (O_2) concentration is important to evaluate the fire risk and update fire-safety strategy in aircraft and spacecraft [5–9]. Once the wire is ignited, the polymer insulation first melts, and then decomposes to release flammable gasses to support the flame. If the polymer insulation melts faster than its burning, the high-temperature molten insulation starts to accumulate, and eventually flows away or drips [10]. Particularly, dripping with a flame can heat and ignite nearby fuels to extend the fire hazard (Fig. 1). Such complex melting and dripping phenomena will also change with the fire size and environmental conditions, but it has not been well studied yet.

Nomenclature

Symbols

A	cross-section area (mm^2)
B	mass transfer number
Bo	Bond number (-)
c	specific heat (kJ/kg/K)
d	diameter (mm)
D	diameter of drip (mm)
g	gravity acceleration (m/s^2)
h	convection coefficient (W/m^2-K)
H	enthalpy (MJ/kg)
ΔH	heat of reaction (MJ/kg)
k	thermal conductivity (W/m-K)
l	length (m)
m	mass (g)
$\dot{m}$	mass-loss rate (mg/s)
M_{dr}	mass of one drip (mg)
Nu	Nusselt number (-)
$\dot{q}''$	heat flux (kW/m^2)
T	temperature (°C)
V_f	flame spread rate (mm/s)
We	Weber number (-)
Y	mass fraction (-)

Greeks

σ	surface tension (Pa)
δ	thickness (mm)
ρ	density (kg/m^3)
λ	thermal conductivity (W/m-K)
μ	dynamic viscosity (Pa·s)
ϕ	equivalence ratio (-)

subscripts

a	ambient
b	burning
c	core
$conv$	convection
dr	dripping
f	flame
g	gas
m	melting
o	outer
O_2	oxygen
p	polymer or preheat
py	pyrolysis
PE	polyethylene

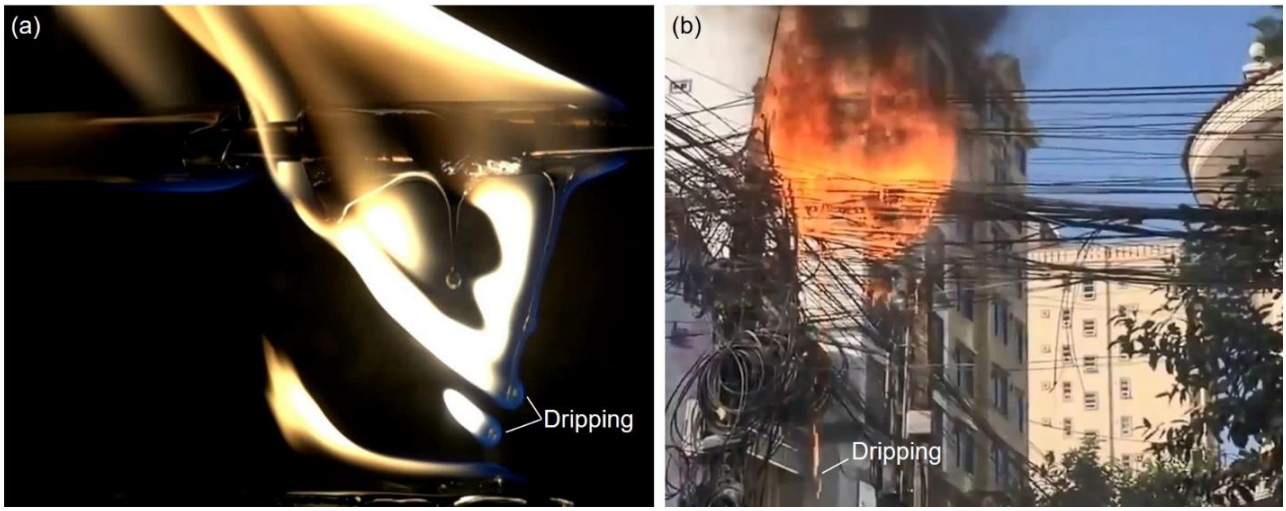

Figure 1. Typical dripping phenomenon from a burning wire: (a) the laboratory wire diameter is 9 mm where the core is made of copper and the insulation is made of polyethylene (see Video 1 in supplemental material); (b) the tangled wires in the street (www.youtube.com/watch?v=-Z0RMFB4H2c)

There are only limited studies on how ambient conditions affect the wire combustion. As pressure is decreased, the rate of flame spread over the thin horizontal wire with nichrome core could increase until near the extinction, because of the increasing diffusion length of flame [7,8]. For copper-core wire, the rate of flame spread has been found to continuously increase with pressure [11,12]. The ignition of wire by a hot coil is easier in a higher O_2 concentration, but becomes more difficult in the reduced pressure [9].

Dripping in wire fire has been reported in past experiments [13,14], and it is often accompanied with a flame, showing a great fire risk. In general, the tendency of dripping is larger for a thicker insulation, while is smaller for a larger core thermal conductance. It has been observed that a larger and heavier drip is required to detach from the core of larger thermal conductivity [15,16]. Also, the dripping behavior in wire fire could be significantly altered by the magnitude and AC frequency of the current [17,18]. As the flame becomes weak in low O_2 concentration, the dripping could act as the heat sink to promote the extinction [19]. Because of the complex nature, the research on the dripping phenomena is very limited. Wang *et al*. [22] studied the dripping behavior of different thermoplastic materials via the UL94 standard test. Kim *et al.* [20,21] simulated the melting, deformation and dripping behaviors of the phase change material (PCM), but the gas-phase flame was not modelled. Huang [10] determined the minimum drip diameter for the flame attachment. However, how the ambient pressure and oxygen level affect the dripping behaviors is still largely unknown.

For electrical wires in different aviation applications (e.g. civil and military aircrafts, drones), their operational ambient pressure could be significantly lower than sea level. Thus, it is not possible to accurately evaluate the aircraft fire safety without considering the risk of flame dripping in wire fire. For this purpose, we conduct a laboratory experiment on thin research wires under different ambient pressures and O_2 concentrations. The flame spread rate, extinction limit and the dripping limited will be quantified in experiment. Then, analysis will be conducted to identify whether the ambient pressure, as well as the O_2 concentration, will promote or prevent the dripping phenomena during the flame spread over thin wires.

2. Experiment

Figure 2 shows the horizontally placed cylindrical cabin which has a diameter of 40 cm and a length of 40 cm. Compared to the past research [7–9], this cabin volume is three times larger, so the effect of O_2 depletion by combustion is much smaller. During the experiment, the cabin is sealed, and the variations of pressure and O_2 are less than 1 kPa and 1%, respectively. The ambient temperature is around T_a = 25℃. The pressure in the cabin can vary from 0.3 kPa to 100 kPa (±0.01 kPa), and the internal pressure is constantly monitored by a pressure gauge. Pure N_2 or O_2 is mixed with air to slowly feed into the pre-vacuumed cabin until the preset pressure level is reached. The ambient O_2 concentration (i.e., mole fraction) varies from 12% to 80%, and additional oxygen sensor is used to monitor the internal oxygen concentration. During the experiment, there is no external airflow inside the cabin.

A task of interest is to study the combined effect of pressure and O_2 level, so a relatively thin special-made research wire, rather than the commercial wire, is used to facilitate this fundamental work on wire combustion. The tested thin research wire has a diameter of $d_o = 0.8$ mm. The soft semi-transparent low-density PE is used as the wire insulation. The PE has a low melting point ($T_m \approx 110$ ℃) and a high pyrolysis point ($T_{py} \approx 387$ ℃, in absent of O_2) [23]. Two core materials are used, copper (Cu) and nichrome (NiCr). The thermal conductivity of Cu is 35 times greater than that of NiCr. Table 1 shows the material thermo-physical properties. The diameter of core metal

is $d_c = 0.5$ mm, and the thickness of PE is $\delta_p = 0.15$ mm, similar to those used in past studies [7–9]. The thin wire is cut into 22 cm samples and placed on the sample holder at the center of the cabin, which is long enough for flame to reach a steady-state spread for all cases, except for those near the extinction limit.

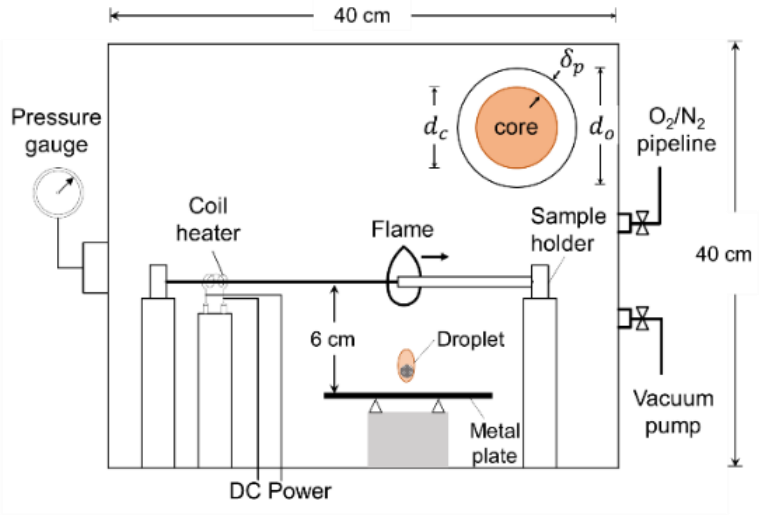

Figure 2. Sketch of the experimental cabin of varying pressure and O_2 level and wire flame spread apparatus.

Table 1. Material properties in the room condition.

Material	k	c	ρ
	W/(m·K)	kJ/(kg·K)	kg/m^3
Cu	398	0.40	8954
NiCr	11.3	0.45	8200
PE	0.23	2.00	918

A coil heater of 15 mm length, placed in one end, is used as the pilot ignition source (6 V and 12 A for 7 s, DC power supply). The whole flame spread process is recorded by a regular digital video camera (30 fps) through the cabin side window. All runs are performed in the darkroom to avoid the noise in images. The dripping flame can be quickly quenched by the metal plate, 6 cm below the wire. The average mass of the dripped molten ball (i.e. a drip) is measured by an analytical balance (± 0.1 mg). At least three tests are repeated for each tested atmospheric condition, and excellent repeatability was observed in the flame spread rate and limiting conditions.

3. Results

3.1. Wire fire phenomena

The typical flame spread processes on a Cu wire at 21% O_2 and 45 kPa are shown in Fig. 3(a). As the pressure decreases, the flame becomes more spherical and bluer, because of the reduction in buoyancy. The top yellow flame becomes small, indicating a lower soot concentration or soot moving away from hotter regions [24]. The flame in reduced pressure becomes spherical and blue, similar to those in microgravity [25].

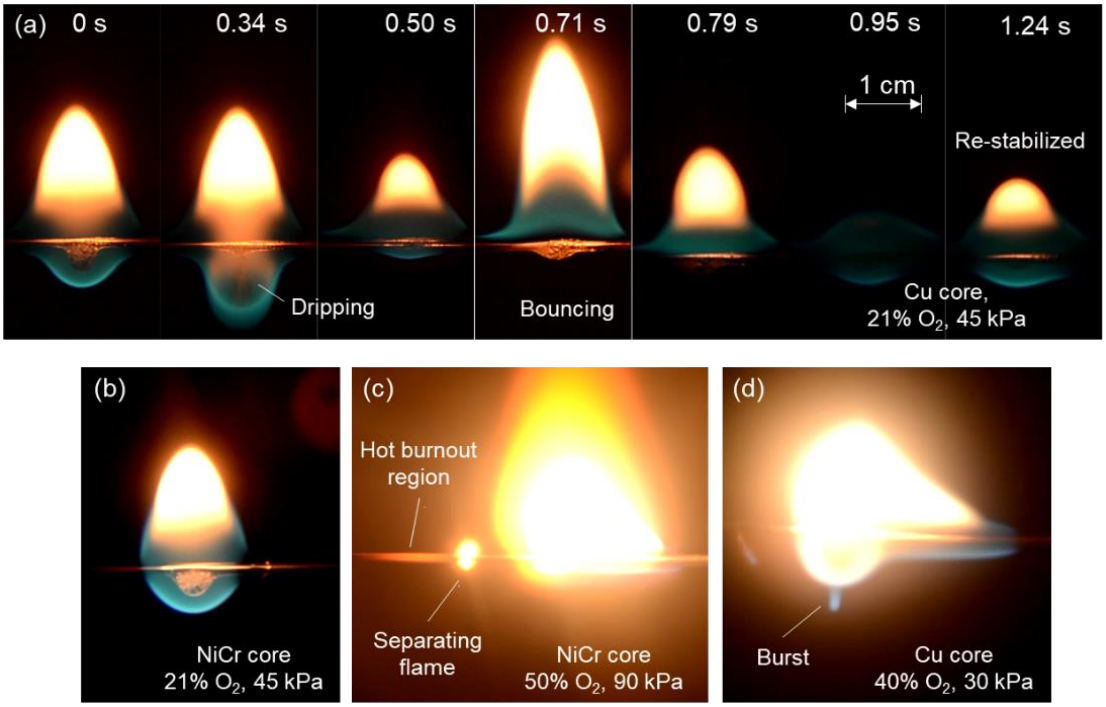

Figure 3. Flame spread phenomena over a thin wire at different ambient conditions, (a) Cu wire (Video 2), and (b) NiCr wire at 21% O_2 and 45 kPa (Video 3), (c) NiCr wire at 50% O_2 and 90 kPa (Video 4), and (d) Cu wire at 40% O_2 and 30 kPa (Video 5).

During flame spread, the solid insulation at the flame leading edge (preheat region) first melts, and then flows into the flame (burning region), accumulating into a ball. There is a mass conservation for the melts generation and consumption,

$$\dot{m}_m = \dot{m}_b + \dot{m}_{dr} \qquad (1a)$$

where $\dot{m}$ is the mass change rate of wire insulaiton; and subscripts *m*, *b*, *dr*, and *r* represent the melting, burning, and dripping, respectively. In this experiment, the polymer remained after flame spread over is negligible. The molten ball hanging below the core is burning/pyrolyzing due to the heating from both flame and core.

Because of dripping, the flame height will change periodically, i.e., the bouncing phenomenon. In Fig. 3(a), after the detach of the molten ball (0.34 s), the flame height decreases because of the removal of fuel. However, the flame can be temporally taller at 0.71 s, which is pushed up by the raising hot product from the dripping flame below. As the molten fuel in the burning zone gradually consumed, the flame reaches the weakest point at 0.95 s. Because the flame continuously heats and melts the fuel in the preheat zone, the flame can eventually re-stabilize itself (Fig. 3a) or extinguish.

Similar phenomena are also observed in NiCr wires (Fig. 3b) and the higher O_2 concentration (Fig. 3c-b). As the O_2 concentration increases, the flame becomes brighter, because of the increased flame temperature and soot concentration. Sometimes, the flame separation occurs in a higher O_2 concentration, if the molten ball is not fully burned and left behind (Fig. 3c). When the core is heated by the hotter flame, the burst phenomenon occurs, i.e., the bubble breaks and the pyrolysates inject through the flame sheet (Fig. 3d).

3.2. Flame spread rate

By tracking the flame leading edge from the video (similar to [7–9]), the mean spread rate (V_f) can be measured. Then, the melting rate of polymer insulation can also be estimated via the linear correlation,

$$\dot{m}_m = \rho_{PE} A_{PE} V_f = \frac{\pi d_o \left(\dot{q}''_{c,p} l_{c,p} + \dot{q}''_{f,p} l_{f,p}\right)}{c_{PE} A_{PE} \left(T_{py} - T_a\right)} \tag{1b}$$

where subscript p represents the polymer insulation or the preheat zone; V_f is the flame-spread rate; ρ, c, A are the density, specific heat, and cross-section area of polymer insulation, respectively; $\dot{q}''$ is the heat flux; and l is the length scale. The convective heating from the flame may be dominant and could expressed as

$$\dot{q}''_f \approx \dot{q}''_{f,conv} = h\left(T_f - T_{PE}\right) = Nu \frac{k_g}{d_o}\left(T_f - T_{PE}\right) \tag{2a}$$

where for the natural convection ($Gr \sim O(1)$), the Nusselt number [26] is

$$Nu = 1.02(Gr \cdot Pr)^{0.15} \propto P^{0.3} \tag{2b}$$

which decreases as the pressure (P) is decreased. Figure 4 summarizes the effect of pressure and O_2 on flame spread rate, where symbols are experimental data and curves are the trend lines, respectively. To help explain, Fig. 5 qualitatively illustrates (a) the heat transfer processes and the core temperature profile, and (b) the effect of ambient O_2 concentration and pressure on the flame spread and dripping. Note that although the ambient pressure and oxygen concentration could modify the pyrolysis temperature of PE, the ambient effect on flame is much stronger and the flame is the primary heating source for pyrolysis. Comparatively, the ambient effect on pyrolysis point should be secondary, and it is not considered in Fig. 5.

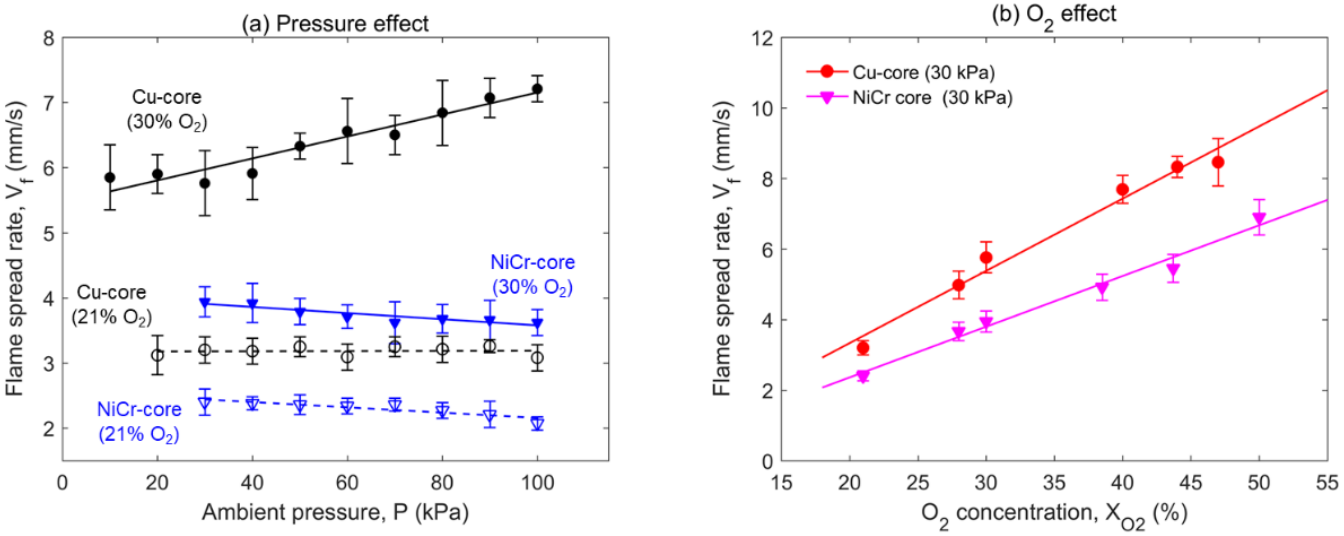

Figure 4. Flame spread rate over Cu and NiCr wires as a function of (a) ambient pressure, and (b) O_2 concentrations, where symbols are experimental data and curves are the trend lines, respectively, and error bars represent the uncertainty of repeating tests.

Previously, Nakamura *et al.* [7] has shown that at 21% O_2, as the ambient pressure was decreased, the flame spread increased for the NiCr wire of a low thermal conductivity, because of a larger flame preheat length ($l_{f,p} \gg l_{c,p}$ and $l_{f,p} \sim D/u \propto P^{-1}$). This finding is also confirmed here using the same NiCr wire (blue dashed line in Fig. 4(a)). Nevertheless, for a larger thermal conductivity core, the preheat length of core ($l_{c,p}$) is larger, which was confirmed recently in [15,16], so the core preheat ($\dot{q}''_{c,p}$) controls the flame spread rate. As illustrated in Fig. 5b, lowering pressure reduces the Gr number, thus, has two compensative effects on the core temperature in preheat region ($T_{c,p}$): (1) decrease it by reducing the flame heat flux in the burning region (Path *cdkp*), and (2) increase it by reducing the convective cooling in the preheat region (Path *clm*). Nakamura *et al.* [7] also showed that for an iron (Fe) core of higher thermal conductivity, there is a balance between these two compensative effects. In this work, we further found that using the Cu core, which has five times greater thermal conductivity of the Fe core, the flame spread rate at 21% O_2 concentration is still invariable with the pressure (black dashed line in Fig. 4(a)), suggesting that the core temperature in the preheat region is still insensitive to the ambient pressure.

Figure 4(a-b) quantifies that as the O_2 concentration increases from 21% to 30%, the average increment in the flame spread rate is 60% for the NiCr wire and 100% for the Cu wire, respectively. Compared to NiCr wire, the additional 40% increment in the Cu wire must come from the core preheating ($\dot{q}''_{c,p}$). In fact, the entire temperature profile of core becomes higher in a higher O_2 concentration, because of the raised flame temperature (T_f) and flame heating ($\dot{q}''_f$) via Path *abk*. In other words, contributions from the hot Cu core and the hot flame ($\dot{q}''_{c,p}$ and $\dot{q}''_f$) to the flame acceleration are comparable. Figure 4(b) also shows that the flame spread increases with O_2 concentration in a linear way. Comparatively, the effect of O_2 is much larger than the pressure, like many other fuels [27].

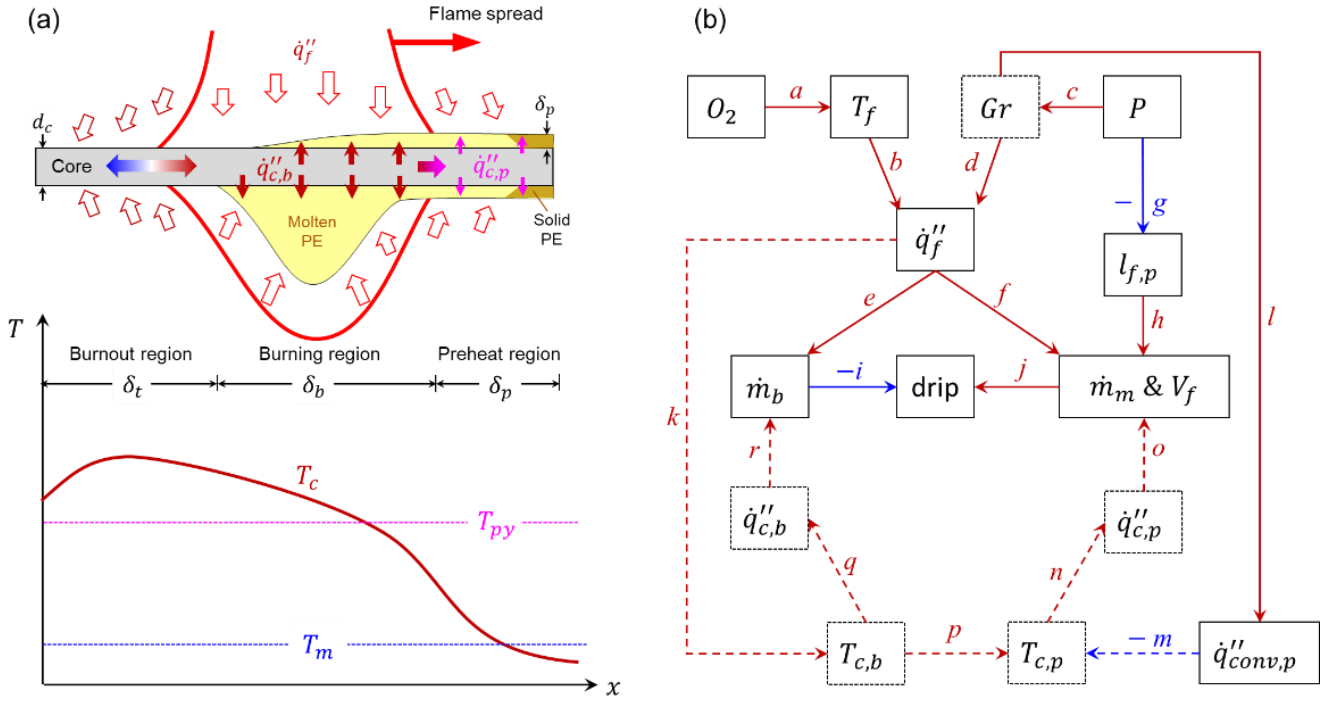

Figure 5. Diagrams for (a) heat transfer process and core temperature profile, and (b) effect of O_2 concentrations and pressure on flame spread and dripping. Subscripts *f, c, p, b*, and *t* represents flame, core, preheat, burning, and burnout, respectively. Red/(-)blue arrow means the positive/negative effect. Dashed arrows represent the core-related effects.

For the NiCr wire (blue solid line in Fig. 4(a)), because of controlled by the flame preheat length flame spread rate in 30% O_2 still increases with decreasing pressure, same as that in 21% O_2. For the Cu wire (black solid line Fig. 4(a)), the pressure dependence of the flame spread rate is still controlled by the core temperature. However, because the increased flame temperature in 30% O_2 provides the additional heat ($\dot{q}_f''$) to the core (Path *abk*), the original balance between Path *cdkp* and Path *clm* in 21% O_2 breaks down. Then, the flame spread rate is controlled by the flame heat flux ($\dot{q}_f''$) and increases with the pressure (Fig. 4). Note that these results may not be extended to a thick wire because different heat transfer components have very different dimension effects.

3.3. Limiting conditions and hazards of wire fire

The dripping occurs when the rate of melting in the preheat zone ($\dot{m}_m$) is larger than the rate of burning in flame ($\dot{m}_b$). In the normal ambience, the flame can spread without dripping. In experiment, by gradually reducing the ambient pressure and O_2 concentration, dripping will occur, and eventually, the flame will extinguish. Additional repeating tests are conducted near the limiting conditions, so that limiting pressure and oxygen levels can be accurately determined. Therefore, there are two limits (dripping and extinction), defining three regions (Fig. 6):

Region A: Flame spread without dripping;

Region B: Flame spread with dripping;

Region C: Extinction.

Two types of extinction phenomena have been observed: (Type I) the flame spread cannot be sustained after the initial ignition state (see Video 6), and (Type II) extinction occurs right after the dripping of molten ball (see Video 7). The Type-I extinction has been discussed in [9], and it takes place near the boundary between Region A and C or when the pressure and oxygen concentration are very low. The Type-II extinction takes place near the boundary between Region B and C.

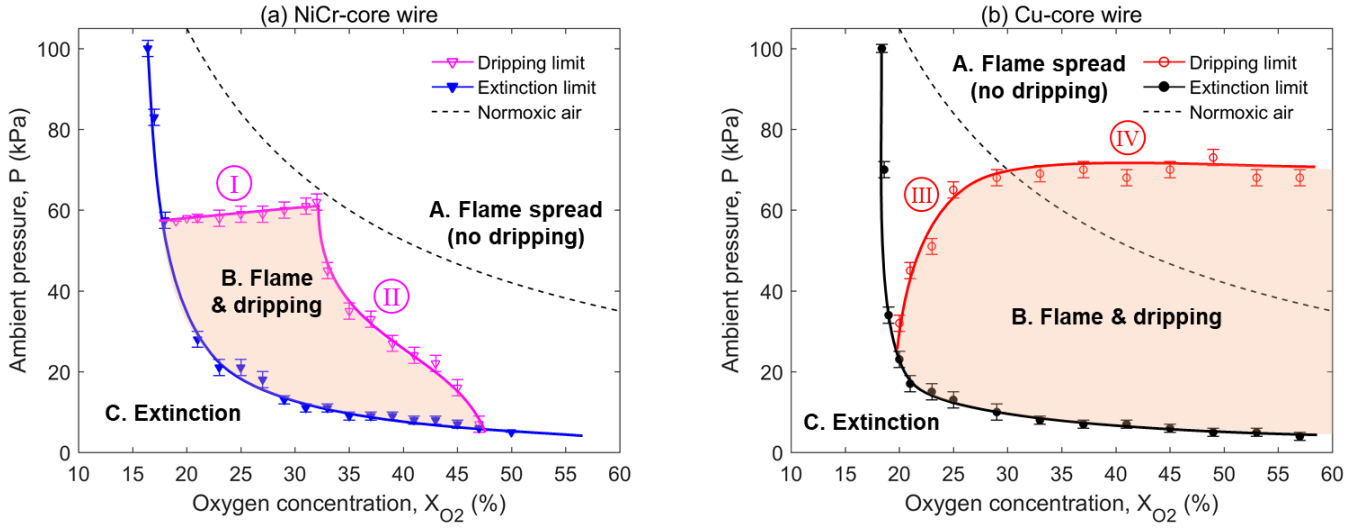

Figure 6. Dripping and extinction limits of (a) NiCr-core wire, and (b) Cu-core wire, where the Normoxic condition (dashed line) means the constant 21 kPa O_2 partial pressure, where error bars represent the uncertainty of repeating tests.

The flame-spread behaviors determine the burning characteristics of wire and fire risk in the direction along the wire. The dripping phenomena determine the potential ignition of nearby objects and the fire risk in the vertical direction. Thus, flame spread and the dripping accompanied with flame represent two different types of wire fire hazards. There is a dual fire-hazard region (between dripping and extinction limits), defining the *worst fire scenario*.

Figure 6 also plots the curve of normoxic air (constant 21 kPa O_2 partial pressure) as a reference. For the Cu wire, following the normoxic condition by reducing the ambient pressure, it may enter the dual fire-hazard region below 70 kPa or above 30% O_2 concentration. Comparatively, no dripping would occur for the NiCr wire throughout the normoxic atmosphere. Thus, attention is needed in choosing the wire material, pressure, and O_2 concentration when a normoxic atmosphere may be required, for example, the future aircraft, aero-spacecraft, and habitats in Moon, Mars and beyond with reduced-gravity [28]. Results in Fig. 6 may not be extended to wires of other dimensions or the spacecraft because dripping phenomenon will not occur in microgravity.

4. Discussions

4.1. Dripping limit

The simple criterion for dripping is the average melting rate larger than the average burning rate, $\overline{\dot{m}_m} > \overline{\dot{m}_b}$, which may be further expressed as

$$\frac{\pi d_o\left(\dot{q}''_{c,p} l_{c,p} + \dot{q}''_{f,p} l_{f,p}\right)}{c_{PE} A_{PE}\left(T_p - T_a\right)} = \overline{\dot{m}_m} > \overline{\dot{m}_b} = \frac{h_f}{c_g}\ln(1+B) \tag{3a}$$

where the average burning rate may be expressed by a mass transfer number (B) [19]

$$B = \frac{Y_{O_2}\left(\Delta H_f/\phi\right) - c_g\left(T_{py} - T_a\right)}{\Delta H_{py} + \left[\left(\dot{q}''_{s,r} - \dot{q}''_{c,b}\right) + \dot{m}''_{dr} H_m\right]/\dot{m}''_b} \tag{3b}$$

where $h_f = \dot{q}''_{f,b}/\left(T_f - T_a\right)$ indicates the flame heating, and $\dot{q}''_{c,b}$ is the heat source.

Figure 6 shows there is a maximum pressure for dripping to occur, 60 kPa for the NiCr wire (Fig. 6a) and 75 kPa for the Cu wire (Fig. 6b). More interestingly, there are two zones, 18~32% O_2 for the NiCr wire (Zone I) and >30% O_2 for the Cu wire (Zone IV), where the dripping limit is fixed at their maximum dripping pressure and is irrelevant to O_2.

For the NiCr wire, the effect of the core on the flame spread and melting is small ($l_{c,p} \ll l_{f,p}$), so the dripping limit should only be controlled by the heating of flame (i.e. $l_{p,f}$ and $\dot{q}''_f$). In Zone I, the dripping occurs only below the maximum pressure, because the *flame heating length* ($l_{f,p}$) is increased to enhance the melting (via Path *ghj*). Increasing the O_2 concentration above 33% (Zone II), the flame temperature (T_f) becomes higher, and the flame heat flux ($\dot{q}''_f$) starts to control the dripping limit. In other words, there may be a *critical flame heat flux*, below which dripping occurs. Thus, the dripping limit is controlled by the compensation between pressure and O_2 concentration, i.e., Paths *ab* and *cd*. Such compensation on flame heat flux also occurs at the extinction limit, so the slope of Zone II is close to that of Extinction limit.

For the Cu wire, the *core temperature* controls the flame spread as well as the melting rate, so there may be a critical core temperature profile (T_c) for dripping to occur. In the low-O_2 Zone III, the reduction in core temperature by increasing the pressure can only be compensated through a raised flame temperature by increasing the O_2. In other words, there is a balance between Path *clm* and Path *abk*. Further increasing the O_2 above 35% (Zone IV), the

already-high flame temperature does not change appreciably. Then, the pressure effect on core temperature in the preheat region ($T_{c,p}$) dominates the dripping limit (via Path *clm*).

4.2. Dripping characteristics

Within the dripping limit, the average mass of a drip was measured by the scale from repeating runs. Because the free fall distance before the drip hits the scale is less than 6 cm, the burning mass loss during the free fall can be neglected. Figure 7 shows that the measured mass of a drip changes appreciably with the ambient pressure and O_2 concentrations, but it is similar between Cu and NiCr wire. The range of drip mass (M_{dr}) is 2~6 mg, which is close to 2~5 mg found in wires of 10 times thicker [15]. Assuming a spherical drip without internal bubbles, its diameter (D) is estimated to be between 1.5 and 2.5 mm, which is larger than the 0.5-mm core in this work and smaller than the 3.5-mm and 5.5-mm core in past experiments [15].

One key observation of this work is that the effect of wire size and the core material on the mass or size of the drip is relatively small. In other words, the size of drip should be mainly controlled by its material properties (e.g., density, surface tension, and viscosity) and flame, rather than the size of the wire.

As illustrated in Fig. 7(d), one criterion for dripping to occur is that the gravity of the accumulated molten ball exceeds its surface tension force

$$M_{dr}g = \rho_{dr}\left(\frac{\pi}{6}D^3\right)g \geq \sigma_{dr}(\pi D) \tag{4a}$$

where ρ_{dr}, D, and σ_{dr} are the bulk density, diameter, and surface tension of molten ball, respectively. Alternatively, it could be expressed by a critical Bond number (or Eötvös number) as

$$Bo = \frac{\rho_{dr}gD^2}{\sigma_{dr}} = 6 \tag{4b}$$

By substituting D, the mass of drip can be estimated as

$$M_{dr} = \rho_{dr}\left(\frac{\pi}{6}D^3\right) = \frac{\pi\sigma_{dr}}{g}\sqrt{\frac{6\sigma_{dr}}{\rho_{dr}g}} \propto \frac{\sigma_{dr}^{3/2}}{\rho_{dr}^{1/2}} \propto T_{dr}^{N} \tag{4c}$$

where N is an index coefficient. Note that the sizes and properties of wire and core do not directly appear in the formula, mainly because the molten ball is hanged at a distance below the wire. The core will still indirectly affect the molten ball via the heat exchange between molten insulation, but such heat exchange should be much smaller than the flame heating.

Figure 7(d) shows that as the molten ball becomes hotter, the surface tension (σ_{dr}) decreases almost linearly [29]. Meanwhile, once exceeding the pyrolysis temperature (T_p), the bubbling phenomenon appears inside the molten ball, which significantly reduces its bulk density (ρ_{dr}). Further increasing the temperature, a strong bursting phenomenon, as found in high O_2 (Fig. 3d), occurs to slow down the decrease in bulk density. Overall, if the change in density dominates, $N > 0$, and if the change in surface tension dominates, $N < 0$. Therefore, increasing its temperature, the mass of a drip can either increase or decrease, depending on the temperature range.

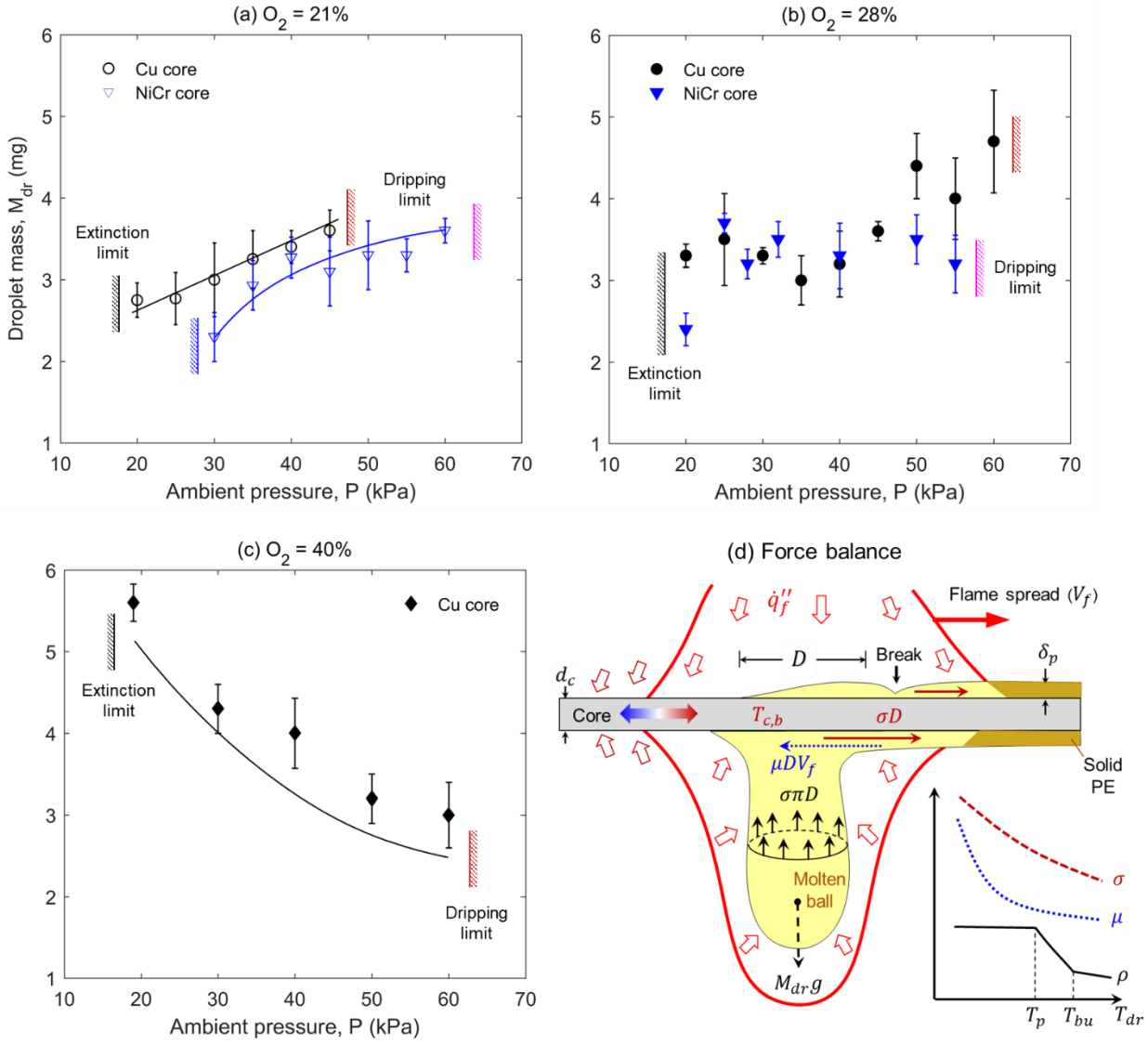

Figure 7. Average mass of a single drip at O_2 concentration of (a) 21%, (b) 28%, (c) 40%, where curves are trend lines, and error bars represent the uncertainty of repeating tests, and (d) diagram for the force balance before the dripping, and the temperature dependence for key thermos-physical properties of the molten ball.

The hanged molten ball is heated by the flame (major) and the core (minor), because of small core diameter. As the pressure increases, the flame heating becomes larger to increase the molten ball temperature. Therefore, if the decrease in density is more prominent ($N > 0$), the mass of a drip may increase as its temperature (or pressure) is increased. Such trend is observed in 21% O_2 (Fig. 7a) and 28% O_2 (Fig. 7b). Further increasing the temperature of the molten ball in a higher O_2, the decrease in surface tension may become dominant ($N < 0$). Then, the mass of a drip may decrease as its temperature (or pressure) is increased, as observed in 40% O_2 (Fig. 7c).

During flame spread, the molten ball moves along with the flame mainly, which is mainly driven by the Marangoni surface tension force. As the continuous heated by the flame, the core temperature gradually increases from the preheat region to burning region (Fig. 5a). Because the surface tension (σ_{dr}) decreases with the increasing temperature, there is a net surface tension force towards the cool preheat zone, which drags the molten ball to follow

the moving flame. This criterion may be expressed as

$$\Delta\sigma_{dr} \geq \mu_{dr} V_f \tag{5}$$

where the Marangoni surface tension ($\Delta\sigma_{dr}$) is proportional to the temperature gradient within the flame, i.e., $\Delta\sigma_{dr} \sim D^{-1}$, and both surface tension and viscosity decrease with temperature (Fig. 7d).

When the O_2 concentration is very high, the flame spread rate (V_f) becomes extremely fast. Then, the surface tension may no longer overcome the inertia of molten ball, breaking the liquid-phase continuity (see Fig. 7d). In other words, the molten ball can no longer catch up with the fast-moving flame. The molten ball, which was left in the hot burnt zone behind the flame, either burned locally (the flame separation in Fig. 3c) or dripped. For a fixed wire dimension, such dripping criterion may be expressed by a critical Weber number (*We*) as

$$We = \frac{\rho_{dr} V_f^2 D}{\sigma_{dr}} \tag{6}$$

which increases significantly with the flame spread rate (V_f). Then, the mass of a drip can be estimated as

$$M_{dr} = \frac{\pi}{6} We^3 \left(\frac{\sigma_{dr}^3}{\rho_{dr}^2 V_f^6} \right) \propto \frac{T_{dr}^b}{V_f^6} \tag{7}$$

where the break point may be surrounding the core, $T_{dr} \approx T_{c,b}$. Regardless of the dependence on its temperature (or the value of *b*), the drip mass significantly increases as the flame spread rate is increased. In a high O_2 concentration, as the pressure increases, the flame spread in Cu wire becomes faster (Fig. 4a). Therefore, the drip mass decreases greatly with the pressure, which also explains with the trend in Fig. 7(c).

For this thin wire (~1 mm), the effect of natural convection should be much smaller than the Marangoni convection. It is because the intensity of natural convection decreases significantly as the size of flow decreases. Comparatively, as the size of flow decreases, the increase of temperature gradient intensifies the Marangoni convection. Moreover, a strong rotation has been observed inside the molten ball, and the Marangoni convection should also be the primary driven force.

In microgravity, although there is no dripping, such detachment (separation) between the fast-moving flame and the molten ball may still occur at the high O_2 concentration, as previously observed in past drop-tower experiments [5]. In addition, there is no natural convection inside the molten layer, so the role of Marangoni convection may become more important. To further verify the dominant force balance in prior to the dripping and investigate the influence of wire dimension, a detailed numerical model are desired in the future research.

4.3. Extinction limit: Core – heat sink or heat source?

One special aspect of wire fire lays in the unique combination of the inner metal core and outer polymer insulation. Whether the core is a heat sink or a heat source in the wire fire has been investigated over the last two decades. For ignition, the metal core acts as a heat sink [9] while for flame spread, the core acts as a heat source [7,8]. Increasing the thermal conductivity and size of the core, the core in the burning zone can change from a heat source which promotes the dripping, to a heat sink which cools molten fuel [15]. Near extinction, core acts as a heat sink because the limit O_2 concentration is higher for the Cu wire [16,19,30]. In fact, if the core thermal conductance is large and the insulation is very thin, the flame cannot be sustained in the wire [14].

Figure 8 replots the extinction limits of Cu and NiCr wires in Fig. 6 as a function of O_2 partial pressure vs. O_2

concentration and total pressure. There is a cross-over point between two wire cores at 18.5% O_2 and 40 kPa, indicating the core changing from a heat source to a heat sink. Below 18.5% O_2, the flame becomes very weak to heat up the core, so the core acts as a heat sink to cool the molten insulation, preventing the pyrolysis. Above 18.5% O_2, the flame in Cu wire can be sustained under a lower pressure than that in NiCr wire. That is, the core becomes a heat source (via Path *clmno*) to compensate for the reduced flame heat flux at a lower pressure. This is the first time that the wire core is found to be both a heat source and a heat sink at the extinction limit.

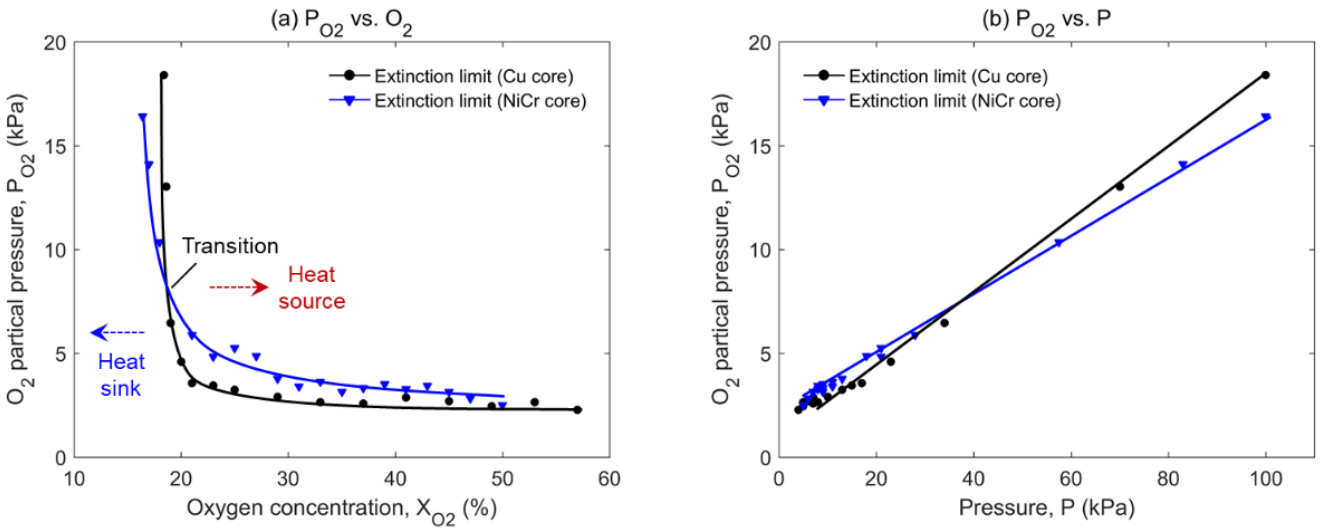

Figure 8. The extinction limit as a function of O_2 partial pressure vs. (a) O_2 concentration, and (b) total pressure.

The linear correlation between O_2 partial pressure and total pressure for extinction or ignition limit has been observed for many materials, such as plastics [31], cellulosic paper [32], and fabrics [33]. Figure 8(b) shows that such linear correlation also exists in both thin wires. Moreover, it suggests that a large change in the solid-phase thermal conductivity can only change the slope, but not the linear trend.

5. Concluding remarks

In this work, we first confirm the flame spread rate in the NiCr wire decreases with increasing pressure in 21% O_2 concentration [7]. and also find such trend extends to a higher O_2 level. In contrast, for the Cu wire, the flame spread rate can increase with increasing pressure because of a stronger core preheat effect.

The spread of a flame and dripping accompanied by a flame represents two different types of fire hazards. For the first time, we find two wire-fire limits, the upper dripping limit and the lower extinction limit, as a function of pressure and O_2 concentration. Between these two limits, both the flame-spread and flame-dripping occur, defining the worst wire-fire scenario. In the "normoxic" atmosphere, dripping occurs to the Cu wire below 70 kPa, but never to the low-conductivity NiCr wire.

The measured mass of a drip is close to that in the wire of ten times thicker [15], i.e., insensitive to the wire size and core material, but it changes with the ambient pressure and O_2 concentration. Analysis of force balance shows that the drip mass is sensitive to its temperature because the density and surface tension have different dependences of temperature. At the extinction limit, we also find that the wire core changes from a heat sink to a heat source by

continuously increasing the O_2 concentration. Despite that the dripping and extinction limits of real wires and in large-scale fires will be very different, these results may still provide valuable implication for designing fire-safe wires used in future aircraft, aero-spacecraft, and human habitats in Moon and Mars.

Acknowledgements

This work was sponsored by the NSFC (51576186, 51636008, 51323010), Key Research Program of the CAS (QYZDB-SSW-JSC029), National Key R&D Program (2016YFC0801504) and Fundamental Research Funds for the Central Universities (WK2320000034, WK2320000036).

References

[1] Government GBD for C and L, Adviser CF& R. Aircraft incidents. London: Stationery Office; 2012.

[2] Baliga BR, T'ien JS. Unsteady effects on low-pressure extinction limit of solid propellants. AIAA Journal 1975;13:1653–6. doi:10.2514/3.7041.

[3] Kleinhenz J, Feier I, Hsu S, Tien J, Ferkul P, Sacksteder K. Pressure modeling of upward flame spread and burning rates over solids in partial gravity. Combustion and Flame 2008;154:637–43. doi:10.1016/j.combustflame.2008.05.023.

[4] Link S, Huang X, Fernandez-Pello C, Olson S, Ferkul P. The Effect of Gravity on Flame Spread over PMMA Cylinders. Scientific Reports 2018;8:120. doi:10.1038/s41598-017-18398-4.

[5] Kikuchi M, Fujita O, Ito K, Sato A, Sakuraya T. Experimental study on flame spread over wire insulation in microgravity. Symposium (International) on Combustion 1998;27:2507–14. doi:10.1016/S0082-0784(98)80102-1.

[6] Fujita O, Nishizawa K, Ito K. Effect of low external flow on flame spread over polyethylene-insulated wire in microgravity. Proceedings of the Combustion Institute 2002;29:2545–52. doi:10.1016/S1540-7489(02)80310-8.

[7] Nakamura Y, Yoshimura N, Ito H, Azumaya K, Fujita O. Flame spread over electric wire in sub-atmospheric pressure. Proceedings of the Combustion Institute 2009;32:2559–66. doi:10.1016/j.proci.2008.06.146.

[8] Nakamura Y, Yoshimura N, Matsumura T, Ito H, Fujita O. Opposed-wind Effect on Flame Spread of Electric Wire in Sub-atmospheric Pressure. Journal of Thermal Science and Technology 2008;3:430–41. doi:10.1299/jtst.3.430.

[9] Huang X, Nakamura Y, Williams FA. Ignition-to-spread transition of externally heated electrical wire. Proceedings of the Combustion Institute 2013;34:2505–12. doi:10.1016/j.proci.2012.06.047.

[10] Huang X. Critical Drip Size and Blue Flame Shedding of Dripping Ignition in Fire. Scientific Reports 2018;8:16528. doi:10.1038/s41598-018-34620-3.

[11] Zhao Y, Chen J, Chen X, Lu S. Pressure effect on flame spread over polyethylene-insulated copper core wire. Applied Thermal Engineering 2017;123:1042–9. doi:10.1016/j.applthermaleng.2017.05.138.

[12] Nakamura Y, Azumaya K, Iwakami J, Wakatsuki K. Scale Modeling of Flame Spread Over PE-Coated Electric Wires. Progress in Scale Modeling, Volume II, Cham: Springer International Publishing; 2015, p. 275–92. doi:10.1007/978-3-319-10308-2_22.

[13] Bakhman N, Aldabaev L, Kondrikov B, Filippov V. Burning of polymeric coatings on copper wires and

glass threads: I. Flame propagation velocity. Combustion and Flame 1981;41:17–34. doi:10.1016/0010-2180(81)90036-5.

[14] Bakhman N, Aldabaev L, Kondrikov B, Filippov V. Burning of polymeric coatings on copper wires and glass threads: II. Critical conditions of burning. Combustion and Flame 1981;41:35–43. doi:10.1016/0010-2180(81)90037-7.

[15] Kobayashi Y, Huang X, Nakaya S, Tsue M, Fernandez-Pello C. Flame Spread over Wires: the Role of Dripping and Core. Fire Safety Journal 2017;91:112–22. doi:10.1016/j.firesaf.2017.03.047.

[16] Kobayashi Y, Konno Y, Huang X, Nakaya S, Tsue M, Hashimoto N, et al. Effect of insulation melting and dripping on opposed flame spread over laboratory simulated electrical wires. Fire Safety Journal 2018;95:1–10. doi:10.1016/j.firesaf.2017.10.006.

[17] Lim SJ, Kim M, Park J, Fujita O, Chung S. Flame spread over electrical wire with AC electric fields: Internal circulation, fuel vapor-jet, spread rate acceleration, and molten insulator dripping. Combustion and Flame 2015;162:1167–75. doi:10.1016/j.combustflame.2014.10.009.

[18] He H, Zhang Q, Wang X, Wang F, Zhao L, Zhang Y. The Influence of Currents on the Ignition and Correlative Smoke Productions for PVC-Insulated Electrical Wires. Fire Technology 2017;53:1275–89. doi:10.1007/s10694-016-0634-y.

[19] Miyamoto K, Huang X, Hashimoto N, Fujita O, Fernandez-Pello C. Limiting Oxygen Concentration (LOC) of Burning Polyethylene Insulated Wires under External Radiation. Fire Safety Journal 2016;86:32–40. doi:10.1016/j.firesaf.2016.09.004.

[20] Kim Y, Hossain A, Nakamura Y. Numerical study of melting of a phase change material (PCM) enhanced by deformation of a liquid–gas interface. International Journal of Heat and Mass Transfer 2013;63:101–12. doi:10.1016/j.ijheatmasstransfer.2013.03.052.

[21] Kim Y, Hossain A, Nakamura Y. Numerical modeling of melting and dripping process of polymeric material subjected to moving heat flux: Prediction of drop time. Proceedings of the Combustion Institute 2015;35:2555–62. doi:10.1016/j.proci.2014.05.068.

[22] Wang Y, Jow J, Su K, Zhang J. Dripping behavior of burning polymers under UL94 vertical test conditions. Journal of Fire Sciences 2012;30:477–501. doi:10.1177/0734904112446125.

[23] Tewarson A. Flammability of Polymers. Plastics and the Environment, Hoboken, NJ, USA: John Wiley & Sons, Ltd; 2004, p. 403–89. doi:10.1002/0471721557.ch11.

[24] Fuentes A, Legros G, Claverie A, Joulain P, Vantelon JP, Torero JL. Interactions between soot and CH* in a laminar boundary layer type diffusion flame in microgravity. Proceedings of the Combustion Institute 2007;31 II:2685–92. doi:10.1016/j.proci.2006.08.031.

[25] Nakamura Y, Yoshimura N, Matsumura T, Ito H, Fujita O. Flame Spread over Polymer-Insulated Wire in Sub-Atmospheric Pressure : Similarity to Microgravity Phenomena. In: Saito K, editor. Progress in Scale Modeling, Springer; 2008, p. 17–27. doi:10.1007/978-1-4020-8682-3_2.

[26] Bergman TL, Lavine AS, Incropera FP, DeWitt DP. Fundamentals of heat and mass transfer, 2011. USA: John Wiley & Sons ISBN 2015;13:470–978.

[27] Fernandez-Pello AC, Ray SR, Glassman I. Flame spread in an opposed forced flow: the effect of ambient oxygen concentration. Symposium (International) on Combustion 1981;18:579–89. doi:10.1016/S0082-

0784(81)80063-X.

[28] Maynard J. NASA Offers $2.25 Million For Martian Habitat Design - How Could This Contest Help People On Earth? Tech Times 2015.

[29] Mendelson RA. Polyethylene Melt Viscosity: Shear Rate-Temperature Superposition. Transactions of the Society of Rheology 1965;9:53–63. doi:10.1122/1.549006.

[30] Takahashi S, Ito H, Nakamura Y, Fujita O. Extinction limits of spreading flames over wires in microgravity. Combustion and Flame 2013;160:1900–2. doi:10.1016/j.combustflame.2013.03.029.

[31] Olson SL, Ruff GA, Miller FJ. Microgravity Flame Spread in Exploration Atmospheres: Pressure, Oxygen, and Velocity Effects on Opposed and Concurrent Flame Spread. 38th International Conference on Environmental Systems, vol. 1, 2008, p. 1–8. doi:10.4271/2008-01-2055.

[32] Nakamura Y, Aoki a. Irradiated ignition of solid materials in reduced pressure atmosphere with various oxygen concentrations – for fire safety in space habitats. Advances in Space Research 2008;41:777–82. doi:10.1016/j.asr.2007.03.027.

[33] Thomsen M, Murphy DC, Fernandez-pello C, Urban DL, Ruff GA. Flame spread limits (LOC) of fire resistant fabrics. Fire Safety Journal 2017;91:259–65. doi:10.1016/j.firesaf.2017.03.072.